Evaluation of different solvents and solubility parameters on the morphology and diameter of electrospun pullulan nanofibers for curcumin entrapment

Lilia M. Guerrini [a*], Maurício Oliveira [a], Camila C. Stapait [d], Milan Maric [b], Amilton M. Santos [c], Nicole R. Demarquette [d]

*guerrini@unifesp.br

[a] *Institute of Science and Technology, Department of Science and Technology, Federal University of São Paulo, São José dos Campos, Brazil.*

[b] *Department of Chemical Engineering, McGill University, Montreal, Canada.*

[c] *School of Engineering of Lorena, Department of Chemical Engineering, São Paulo University, Lorena, Brazil.*

[d] *Department of Mechanical Engineering, École de Technologie Superieure (ÉTS), Montreal, Canada*

Abstract: In this work, the effect of different solvents and solvent binary mixtures on the morphology of electrospun pullulan (Pull) nanofibers was evaluated. The solution viscosities, interactions between solvent and polymer, as well as, solvent vapor pressure, were correlated to the morphology and diameters of the nanofibers. Water, dimethylformamide (DMF) and dimethyl sulfoxide (DMSO) and Teas graphs that rely on the use of Hildebrand solubility parameters were used to identify the most suitable mixtures of solvents. The best binary mixture of solvents to produce Pull nanofibers without defects and with small diameters (203±32 nm) was DMF/DMSO in the ratio of 70/30 wt.%. Pull nanofibers containing 3 and 5 wt. % of curcumin (Curc) in a mixture of DMF/DMSO (70/30 wt.%) were then obtained, and the entrapment efficiency was evaluated using ^{1}H NMR and a UV-vis spectrophotometer. The results obtained in this work create a new approach for the production of Pull nanofibers for drug delivery systems.

Keywords: Pullulan, Hansen solubility parameter, Solvent mixture, Electrospinning, Curcumin

1. Introduction

Pullulan (Pull) is a linear polysaccharide produced in large scale from starch, glucose and some agro-industrial waste by the fungus *Aureobasidium pullulans* (Bauer, 1938; Bender Lehmann & Wallenfels, 1959; Hilares et al., 2019; Leathers, 2003; Sugumaran & Ponnusami, 2017; Tabasum et al., 2018;). It consists of maltotriose units, α (1,4) connected glucose that are linked via α(1,6) glycosidic bonds (Leathers, 2003, Singh, Kaur, & Kennedy, 2015; Swn, Kim, Lee, Cho, & Bvum., 1989). Its structure is showed in supplementary material Fig. S1. The regular alternation of these bonds is responsible for several properties of Pull such as high solubility in water, oxygen barrier, non-toxicity, non-carcinogenicity, non-mutagenicity, and biodegradability (Prajapati, Jani, & Khanda, 2013; Rekha & Sharma, 2007).

Pullulan has been used in several applications such as blood plasma substitutes, oil and oxygen barrier films, bio-based phase change materials, additives for food, cosmetics and adhesives (Balderrama, Dourges, Magueresse, Maheo, & Deleuze, 2018; Cheng, Demirci, & Catchmark, 2011; Kumar, Saini, Pandit, & Ali, 2012; Leathers, 2003; Rekha & Sharma, 2007; Prajapati et al., 2013; Oguzhan & Yangilar, 2013). Emerging markets propose its use in cancer therapy as a carrier and releaser of cytotoxic molecules, drug capsules for vegetarians, diabetics, and patients with restricted diets (Cheng et al., 2011; Ganeshkumar, Ponrasu, Subamekala, Janani, & Suguna, 2016; Jo et al., 2007; Kumar et al., 2012; Prajapati et al., 2013).

Due to these very interesting properties, Pull is an interesting candidate to obtain electrospun nanofibers made out of nanofibers to be used in several biomedical applications such as drug delivery. In electrospinning, a high voltage is applied to a polymer, which can be in the form a polymer solution or a molten polymer. The electrostatically charged polymer is stretched into fibers, in the nano-to-micro-meter scale range, which are collected on a grounded target, called a collector. The resulting material forms a nonwoven scaffold whose large surface area is valuable for applications in biomedical tissue engineering. In the electrospinning process, the properties of the nanofibers, governed by their morphology, are controlled by the polymer properties such as molar mass, molar mass distribution, structure of the polymer (linear or branched chains), polarity, solvent vapor pressure and electrical properties, polymer solvent interaction that can be assessed by the Hildebrand solubility parameters, and processing parameters (solution flow rate, electrical field and emitter collector distance) (Guerrini, Oliveira, Branciforti, Custódio, & Bretas, 2009; Han, Yarin, & Reneker, 2008; Luo, Stride, & Edirisingh, 2012; Senthil & Anandhan, 2013). In particular, the selection of a solvent or a solvent mixture has a significant influence on the electrospinnability, morphology of the nanofibers (large variation on the fiber diameter, presence of defects like beads or junctions, pores in the fibers and so on), and membranes mechanical

properties (Lubasova & Martinova, 2011; Luo et al., 2012; Mahalingam, Raimi-Abraham, Craig, & Edirisinghe, 2015; Senthil & Anandhan, 2013). The selection of this solvent should take into account its affinity to the polymer to be electrospun, its vapor pressure and electrical properties.

Pull has very poor solubility in organic solvents except for dimethylformamide (DMF) and dimethylsulfoxide (DMSO) (Leathers, 2003; Pereira, 2013; Sugumaran & Ponnusami, 2017; Tsujisaka & Mitsuhashi, 1993). However, it is expected that if different solvents or mixtures of solvents are used to obtain solutions for electrospinning, different fiber morphologies may be obtained and help in obtaining small diameter fibers that are of the utmost importance for drug delivery. Up to date, to our knowledge, very few studies have been published on the electrospinnability of Pull (López-Rubio, Sanchez, Wilkanowicz, Sanz, & Lagaron, 2012; Stijnman, Bodnar, & Tromp, 2011) and no study reported the influence of solvent choice on fiber morphology. In the present work, the influence of Pull molar mass, various solvents, and solvent mixtures, on the electrospinnability, morphology, and the potential of Pull fibers to be used for drug delivery was studied.

A practical way to predict polymer solubility of a polymer in a given solvent consists of evaluating Hildebrand solubility parameters (δt) (Hildebrand & Scott, 1962) that can be written as the sum of three components known as Hansen solubility parameters (HSP): the polar force component (δ_p), the dispersion force component, (δ_d) and the hydrogen bonding component (δ_h), as described by Eq. (1) (Hansen, 1967c, 1967b, 1967c; Lubasova & Martinova, 2011; Mahalingam et al., 2015).

$$\delta_t^2 = \delta_p^2 + \delta_d^2 + \delta_h^2 \qquad\qquad \text{Eq. (1)}$$

Hansen solubility parameters can be used to predict the interactions between two polymers or between a polymer and a solvent employing a graphical method (Hansen, 1967c, 1967b, 1967c). This method consists of using a triangular graph, known as a Teas diagram (Luo, et al., 2012; Mahalingam et al., 2015) having on each of its axes the values of fractions of the Hansen parameters (*f*) given by Eq. 2.

$$f_d = \frac{\delta_d}{\delta_d + \delta_p + \delta_h}\ , f_p = \frac{\delta_p}{\delta_d + \delta_p + \delta_h}, f_h = \frac{\delta_h}{\delta_d + \delta_p + \delta_h} \qquad \text{Eq. (2)}$$

A point for each solvent and polymer can then be placed on the diagram. Then, the composition of an ideal solvent mixture for the polymer can be found using a logic that is similar to the ones used to read phase diagrams (Luo et al., 2012). Teas diagrams were used in the present work to evaluate the electrospinnability of Pull in different solvent mixtures following the work of Luo, Stride & Edirisinghe, 2012, who studied the electrospinning of polycaprolactone (PCL) and Mahalingam et al., (2015) who produced nanofibers of poly (butylene terephthalate) using pressured gyration as spinning.

The possibility of obtaining fibers as well as certain fiber diameters were related to the solution viscosities and Pull molar masses, as well as, the interactions between solvent and polymer, solvent vapor pressure, and electrical properties. Water, DMF and DMSO and solvent mixtures of H$_2$O/DMSO, H$_2$O/DMF, DMF/H$_2$O and DMF/DMSO were used. Aiming at future drug delivery applications, the addition of curcumin, which is a potent antioxidant, antibacterial, reactive oxygen species scavenger, and anti-inflammatory agent (Ganeshkumar et al., 2016; Yakub et al., 2020b, 2020b), was also evaluated.

2. Experimental

2.1 - Materials

Pullulan (Pull, cosmetic grade, Hayashibara Co., Japan) was fully dissolved in deionized water, dialyzed in deionized water for 2 days (MWCO of 14000 kDa, Spectra/Por®), precipitated in ice-cold methanol, filtered and then dried under vacuum at 30°C for 24 h prior to use. Deuterated dimethyl sulfoxide (DMSO-d$_6$, >99.9 %), *N,N*-dimethylformamide HPLC grade (>99.9 %), lithium bromide (LiBr, ≥99 %) and hydrochloric acid (HCl, 37 %) used for ^{1}H NMR spectroscopy and chromatography analysis were obtained from MilliporeSigma. Dimethyl sulfoxide (DMSO, >99.9 %, Fisher Scientific) and *N,N*-dimethylformamide (DMF, >99.9 %, MilliporeSigma) were dried over molecular sieves (3 Å, MilliporeSigma) to be used as solvents for the electrospinning process. Curcumin (Tumeric Rhizome, Curc, >95 %) was supplied by Fisher Scientific and was used without further purification. Deionized water (DW) with a conductivity of 1.1 µS/cm was used throughout the study.

2.2. Pullulan molar mass reduction

In order to understand the effect of Pull molar mass on the processing parameters and nanofiber morphologies, the purified Pull was treated with 0.025M hydrochloric acid solution (HCl) to obtain different molar masses (Ilić, Jeremi, & Jovanovi, 1991; Shady et al., 2013). In a dry 200 mL three-neck round bottom flask, purified Pull (4.0 g) was dissolved in HCl solution (80 mL, 0.025 mol/L) under a magnetic stirrer and under nitrogen atmosphere. The flask was heated at (85±1) °C for different amounts of time (from 0 to 2.5h). The reaction was stopped by putting the flask in an ice bath and then the product was obtained by precipitation into ice-cold methanol, and then washed with cold methanol several times, filtered and dried under vacuum at 30 °C for 24 h. The weight-average molar mass ($\overline{M}_w$), number-average molar mass ($\overline{M}_n$) and the dispersity index ($Đ=\overline{M}_w/\overline{M}_n$) were measured by size exclusion chromatography (SEC, Waters Breeze) with

HPLC grade DMF with 1.0 g/L of LiBr as the mobile phase running at a flow rate of 0.3 mL/min at 50 °C. The SEC is equipped with a guard column and with 3 Waters Styragel HR columns where the molecular mass ranges are given, and a differential refractive index detector (RI 2410). Pull dried sample were dissolved in HPLC DMF at a concentration of 10 mg/mL, and then filtered through a 0.45 μm pore-size polytetrafluoroethylene (PTFE) syringe filter before analysis. The relative molar masses were evaluated from a calibration based on monodisperse poly (methyl methacrylate) (PMMA) standards, with molar mass (HR 1 with a range of 100 to 5,000 g/mol, HR 2 with a range of 500 to 20,000 g/mol and HR 4 with a range of 5,000 to 600,000 g/mol) (Varian).

2.3. Pullulan solution preparation

Pull solutions were prepared in three different solvents (H₂O, DMF, DMSO) and several of their binary mixtures (H₂O/DMSO, H₂O/DMF, DMF/DMSO). Pullulan was solubilized in 34 g of the solvent or binary mixture in a 50 mL three-neck round bottom flask, with a magnetic stirrer at 40 °C. The total Pull and Pull/curcumin solution concentration was fixed at 15wt.% and was confirmed by means of gravimetric analysis at 100°C. The processing conditions that resulted in the fibers with the best morphologies were used to evaluate the possibility of using Pull fibers in drug delivery. For that, two homogeneous solutions containing 3 and 5 wt.% of curcumin were prepared. Pullulan (2.91 g) was dissolved in 17.0 g of DMF/DMSO mixture (70:30 wt.%) with a magnetic stirring at 40 °C for 1 h and to this solution, 0.09 g (0.244 mmol) of Curc was added under vigorous magnetic stirring, resulting in a final Curc concentration of 3 wt.%. The same procedure was repeated with 2.85 g of Pull and 0.150g (0.407mmol) of Curc to obtain Curc concentration of 5 wt.%.

2.3.1. Pullulan solution characterization

In order to understand the parameters controlling the electrospinning process of polymer solutions, the rheological behavior of the 15wt.% Pull solutions was evaluated using a rotational rheometer (Anton Paar, MCR 302) equipped with cylindrical concentric geometry (CC17). The viscosity was measured for shear rates ranging from 0.1 to 1,000 s⁻¹ at (24 ±1) °C. The results were obtained in duplicates and the average values are reported in this work. The Hansen solubility parameter (HSP) and fractional solubility parameters for each solvent and Pull were calculated and used for building the Teas graph that enables identifying the solvent mixture that would result in the best solubility for Pull. The solubility parameters of Pull were calculated based on the Van Krevelen & Nijenhuis (2009) method, using Eq. (4) and the values reported in Table 1. The fractional solubility parameters (f_d, f_p, f_h) were determined by the relative amounts of the three component forces following Eq. (2). The vapor pressure (P_{vi}), boiling temperature (T_{bi}) and

dielectric constant (ε_i) of the solvent mixtures were calculated by Eq. (3) using the values of H_2O, DMF and DMSO from literature (Smallwood, 1996; Mark, 1999). These values and the calculated values are reported in Table 3.

$$P_{vmixture} = \Sigma P_{vi}\phi_i, \quad T_{bmixture} = \Sigma T_{bi}\phi_i, \quad \varepsilon_{mixture} = \Sigma \varepsilon_i \phi_i \qquad \text{Eq. (3)}$$

$$\delta_d = \frac{\Sigma F_{di}}{V_m}, \quad \delta_p = \frac{\sqrt{\Sigma F_{pi}^2}}{V_m}, \quad \delta_h = \sqrt{\frac{\Sigma E_{hi}}{V_m}} \qquad \text{Eq. (4)}$$

where: E_{hi} = cohesive energy of hydrogen bonding forces, F_{di} = dispersion forces, F_{pi} = polar forces, i = contributing group, V_m = molar volume of polymer and ϕ_i = fractions of the solvents.

Table 1. Structural groups estimated in this work used to determine Hansen solubility parameters of the Pull.

Structural groups	Number of groups (N)	N.Fd$_i$ (J$^{1/2}$cm$^{3/2}$/mol)	N.F^{2}p$_i$ (J.cm^3/mol)	N.Eh$_i$ (J/mol)
-OH	9	1890	2250000	180000
-O-	6	600	2400	18000
-CH$_2$-	3	810	0	0
=CH-	15	3000	0	0
Σ		6300	2252400	198000

2.4. Electrospinning

The nanofibers of Pull and Pull/Curc were produced using a pilot-scale electrospinning device (Fluidnatek® LE-100) from Bionicia (Valencia, Spain). The electrospinning setup consisted basically of a high voltage power supply, static metallic collector covered with aluminum foil, a 10 mL glass syringe along with a stainless-steel needle (23G) containing the polymer solution, and a pump for controlled solution flow rate. The processing parameters used were: electrical voltage varying from 20 to 24 kV while keeping the flow rate at 0.5 mL/h, the working distance between the needle and the collector was set at 17 cm, the temperature and relative humidity were set at (24.0 ± 0.5) °C and (60 ± 0.3) % respectively. For solutions containing 3 and 5 wt.% of Curc (Pull/Curc), the process parameters were the same as those used for electrospinning of Pull solutions. For the solutions with Pullulan with reduced molar mass a 26G needle was used.

2.4.1. Nanofibers characterization

The electrospun fibers were characterized by scanning electron microscopy (SEM-Hitachi S3600N). After being coated with gold by sputtering (K550X Quorum Technol. K550X), the morphology and homogeneity of the fibers were observed using a SEM. The average diameter of

the nanofibers was measured using the image analysis software (Image J). In order to represent the diameter distribution and the average diameters, 100 different fibers were measured from each sample and the average values were presented. For determining the Curc entrapment efficiency (CEE) into Pull-Curc nanofibers, accurately weighed nanofiber mats were placed in DMSO and analyzed by a UV-vis spectrophotometer (Thermo, Evolution 260 Bio), based on predetermined calibration for Curc at a wavelength of 426 nm (Rezaei & Nasirpour, 2019). For this, 2.5 mg of the nanofiber mats was dissolved in 5 mL of DMSO under magnetic stirring during 1h and the obtained solution was diluted 15 times and then analyzed. The CEE was calculated according to the feed ratio of the actual to theoretical Curc content in the nanofibers (Eq. 5).

$$CEE(\%) = \left(\frac{C_R}{C_L}\right) x 100 \qquad (5)$$

where: C_R represents the real amount of Curc, which was determined from the fibers and C_L is the amount of Curc loaded for the preparation of fibers mat.

The determination of entrapped Curc into Pull-Curc nanofiber mat was also done in duplicates by proton nuclear magnetic resonance (^{1}H NMR) in dimethyl sulfoxide (DMSO-d$_6$) using a Bruker AVIIIHD Spectrometer at a field frequency of 500 MHz and 16 scans at 30 °C. The amount of Curc was evaluated considering the integration of the peak of the acetyl group (-OCH$_3$-), which was observed at approximately 3.86 ppm and the integration of the backbone protons in the 4.45 – 5.6 ppm region, considering the protons in the Pull repeat unit.

3. Results and discussion

3.1. Effect of molar mass on the Pull electrospinning

Table 2 shows the weight-average molar mass ($\overline{M}_w$), number-average molar mass ($\overline{M}_n$) and the dispersity ($Đ=\overline{M}_w/\overline{M}_n$) obtained for Pull after molar mass reduction as a function of reduction time.

Table 2. Molar masses ($\overline{M}_w$ and $\overline{M}_n$) and dispersity ($Đ$) of Pull with different reduction times.

Reduction time (h)	$\overline{M}_w$ (g/mol)	$\overline{M}_n$ (g/mol)	$Đ$
0.0	91,000	42,700	2.13
0.5	60,000	28,800	1.80
1.0	20,000	11,330	1.70
2.0	12,650	7,500	1.70
2.5	10,500	6,560	1.60

From the results shown in Table 2, it can be seen that the molar reduction method used in this work was efficient as the molar mass of Pull decreased almost 9 times in comparison to the one of standard Pull. The molar mass ($\overline{M}_w$) of Pull decreased from 91,000 g/mol to 10,500 g/mol after 2.5 h of acid treatment. Willersinn, Bogomolova, Cabré, and Schmidt (2017)also evaluated molar mass reduction after HCl treatment of pullulan and related this reduction to cleavage of α-(1,6) bonds between the maltotriose units.
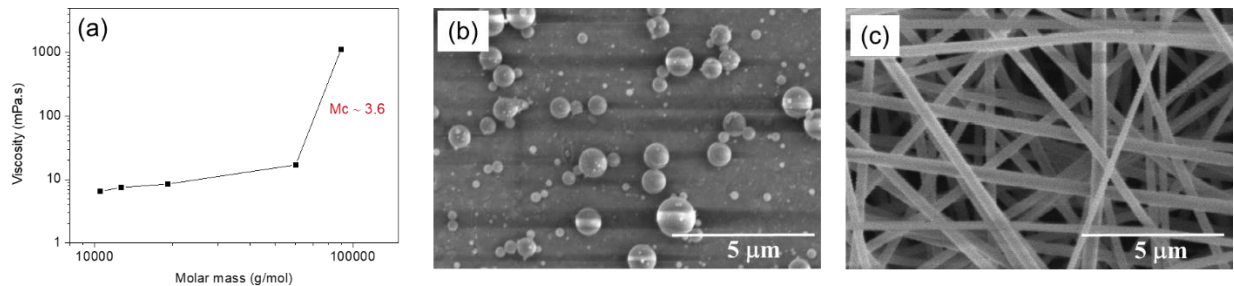

Figure 1. Viscosity versus $\overline{M}_w$ of Pull/water solutions (a), morphology of the electrospun Pull/water as a function of $\overline{M}_w$= 20,000 g/mol (b) and $\overline{M}_w$= 91,000 g/mol (c).

Fig. 1a presents the viscosity of the solutions as a function of molar mass of Pull. Two regimes can be observed: for molar masses below 20,000 g/mol, the viscosity increases slightly with molar mass whereas it increases sharply for molar masses above 60,000 g/mol, for molar masses above 60,000 g/mol. The $\eta_0 \sim M_c^{3.6}$ which corresponds to the dependency of viscosity on molar mass once the molar mass is above molar mass of entanglement.

Fig. 1b and c present the morphologies that were obtained by electrospinning solutions of Pull with molar masses below 60,000 g/mol and above this value, respectively. In this case, it is for $\overline{M}_w$= 91,000 g/mol and $\overline{M}_w$ = 20,000 g/mol, respectively. For Pull weight-average molar mass below 60,000 g/mol, only particles were obtained (electrosprayed particles). Low molar mass does not allow the formation of enough entanglements between the polymer molecules, or enough viscoelastic forces to stretch the drop during electrospinning to produce nanofibers, independently of the processing conditions (voltage was varied from 15 to 24 kV). For molar masses above 60,000 g/mol, for which there are enough entanglements formed between the polymer molecules, a relationship similar to $\eta_0 \sim M_c^{3.6}$ was observed. The presence of entanglements enabled obtaining fibers when the molar mass of Pull was 91,000 g/mol. In that case, fibers with an average diameter of 340 nm were obtained. The results presented here are similar to those obtained by López-Rubio et al. (2012); Stijnman et al. (2011) and Sun, Williams, Hou, and Zhu (2013) who were able to electrospin Pull with a molar mass above 100,000 g/mol. They obtained fibers with diameters ranging from 274 to 548 nm which is in good agreement with the diameter obtained in this work.

3.2. Effect of solvents on the Pull solution electrospinning

Fig. 2 presents the Teas graph that was used to evaluate the best mixtures of solvents which were identified to be 40/60 wt. % for H_2O/DMSO, 30/70 for H_2O/DMF and 20/80 for DMF/DMSO. The ideal solvent mixtures were selected from the Teas graph using a geometric method similar to the lever rule as reported by Luo et al. (2012). A line was drawn and measured using a ruler between the polymer and each solvent to calculate the fractions of the ideal mixture by the lever rule.
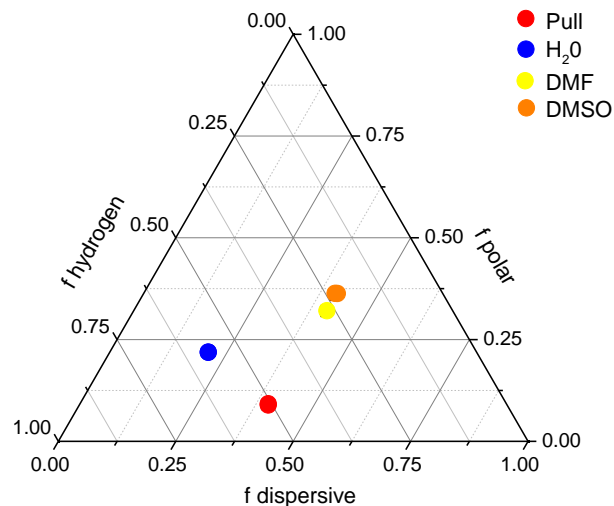

Figure 2. Teas graph of fractional solubility parameters for Pull, H_2O, DMF and DMSO.

The Teas graph shows that Pull has high amount of hydrogen interactions. The major difference among water, DMF and DMSO is related to hydrogen interactions. Water has the highest value of this interaction and also is the closest solvent of the Pull.

Fig. 3 presents typical morphologies of Pull fibers obtained in this work. In this case, fibers obtained from a solution 15 wt.% Pull solution in DMF, as well as, from a solution with 70/30 and 30/70 wt.% H_2O/DMF respectively are shown. The morphology of all electrospun Pull at 20 and 24 kV are showed in Figs. S2-S3.
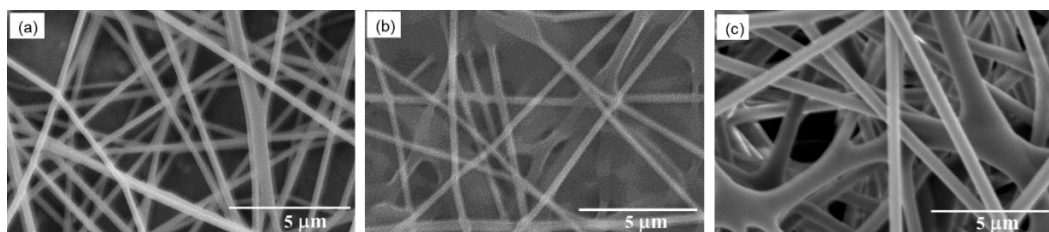

Figure 3. SEM morphology of Pull fibers produced at 20 kV from the following solutions. (a) Pull/DMF, (b) Pull/H_2O/DMF (70/30 wt.%) and (c) Pull/H_2O/DMF (30/70 wt.%).

It can be seen that for the solution with Pull/DMF regular fibers without defects were obtained. Similar results were obtained for Pull/H_2O, Pull/H_2O/DMSO and Pull/DMF/DMSO

9

with 30 wt.% of DMSO in the solvent mixture. Conversely, when the used solvent was H_2O/DMF with 30 wt.% of DMF, junctions with fibers and also polymer films were observed (Fig. 3b). This behavior could be improved when 70 wt.% of DMF was used (Fig. 3c). However, in this case some junctions between the fibers were observed. It was not possible to obtain Pull fibers when 40/60 of H_2O/DMSO, 30/70 for H_2O/DMSO, 20/80 for DMF/DMSO and 100 wt.% of DMSO were used as solvents. It is important to highlight that, based on the results obtained from the Teas graph estimation, the proportion of 70/30 wt.% was chosen for the binary solvents to evaluate the best conditions to produce nanofibers without defects by electrospinning.

Table 3 presents the diameters, as well as, the solvent constants, as calculated using Eqs. 3 and 4, for all the solutions tested in the present work. The results highlighted in grey correspond to the solvent concentrations found using Teas diagram.

Table 3. Diameters of fibers obtained using different combinations of solvents
(20 kV, 1.2 kV/cm, 0.5 mL/h, 24°C, 60 % RH).

H_2O/DMF	100/0	70/30		30/70	0/100
T_b (°C)	100	116		137	153
P_v (25 °C) (mmHg)	23.8	17.8		9.9	3.9
ε (20 °C)	79.7	66.8		49.6	36.7
δ_t [Mpa$^{1/2}$]	47.8	40.9		31.7	24.8
η (mPa.s)	1130	2255		4000	5350
$\emptyset$ (nm)	302±50	320±101		597±154	294±37
Appearance	Fibers	Fibers+junctions+film		Fibers+junctions	Fibers
H_2O/DMSO	100/0	70/30	40/60	30/70	0/100
T_b (°C)	100	126.7	153.4	162.3	189
P_v (25 °C) (mmHg)	23.8	16.8	9.9	7.5	0.6
ε (20 °C)	79.7	69.8	60	56.6	46.7
δ_t [Mpa$^{1/2}$]	47.8	41.5	35.1	33.0	26.7
η (Pa.s)	1130	2260	5100	8980	20700
$\emptyset$ (nm)	302±50	546±82	Not possible	Not possible	Not possible
Appearance	Fibers	Fibers	Film	Film	No fibers
DMF/DMSO	100/0	70/30		20/80	0/100
T_b (°C)	153	164		181.8	189
P_v (25 °C) (mmHg)	3.9	2.9		1.3	0.6
ε (20 °C)	36.8	39.8		44.7	46.7
δ_t [Mpa$^{1/2}$]	24.8	25.4		26.3	26.7
η (Pa.s)	5350	10940		11660	20700
$\emptyset$ (nm)	294±37	220±30		Not possible	Not possible
Appearance	Fibers	Fibers		Film	No fiber

It can be seen from Table 3 that the best polymer/solvent affinity (as calculated using Teas diagram) does not necessarily result in the best processability. Similar conclusions were drawn by Luo et al. (2012) who studied the electrospinnability of PCL. They showed that the use of solvents with strong van der Waals forces, strong hydrogen bonding, and weak polar forces, presenting high affinity with PCL, resulted in obtaining large electrosprayed particles and did not enable electrospinning. However, the use of solvents presenting a partial to high solubility with moderate dispersion forces frequently resulted in good electrospinnability. The results reported here indicate that the quality of the electrospun mats significantly depends on the viscosity of the solution, vapor pressure, and electrical properties of the solvents. All the tested solutions had a viscosity above 1000 mPa.s resulting in the formation of enough entanglements, which are necessary to obtain fibers. However, when DMSO was used in concentrations varying from 60 to 100%, only films were obtained. This can be explained by the high boiling point and the lower vapor pressure of DMSO. Similar results were reported by Kong & Zieger (2014) who could not electrospin fibers with a solution from Pull/H_2O/DMSO with a high amount of DMSO.

When water was used to electrospin Pull, fibers without defects were obtained. However, when 30 wt.% of DMF was added to the solution, the behavior in the electrospinning process changed resulting in a morphology with films and fibers. This mixture presents good solvent interactions, and the viscosity is 2255 mPa.s. The vapor pressure (17.8 mm Hg) of this mixture and boiling temperature (116 $^{\circ}$C) are close to that of water. However, in spite of the high viscosity value, good solvent interactions, and a moderate decrease of the vapor pressure compared to that of pure water, the use of a 70/30 water/DMF solution resulted in polymer fibers with many defects. Most likely the presence of DMF together with water affected the evaporation of the solvent affecting the morphology of the mat obtained even if these solvents are miscible. A more defined morphology was obtained when 30/70 wt.% water/DMF solution was used. This ratio was estimated by the Teas graph as the best solubility interactions for these solvents. The viscosity value and boiling point are higher (4000 mPa.s and 137 $^{\circ}$C), and the vapor pressure is lower (9.9 mmHg) than that of water and the mixture in the ratio of 70/30 wt.%. In spite of that, the solution has enough force to stretch, to form a jet, and to evaporate the solvents to produce fibers. However, due to the instability of the formed jet, these fibers exhibit some junctions. These fibers were, also, considered, and their diameters were found to be around 597 nm.

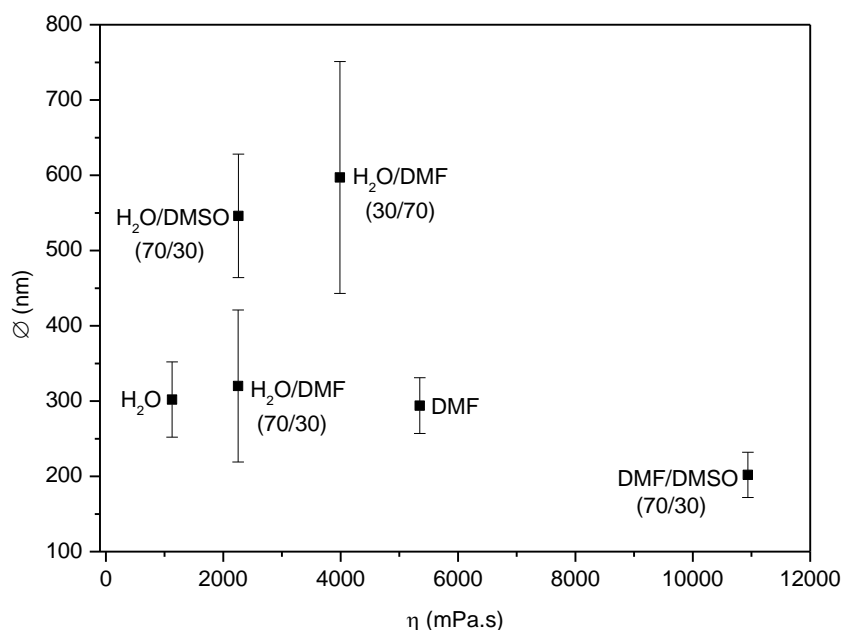Figure 4 shows the diameter of the fibers as a function of solution viscosity.

Figure 4. Fiber diameter (20 kV) versus solution viscosity from different solvents.

It can be seen that the diameter of the fiber was not affected by the value of the viscosity for both H_2O/DMF and DMF/DMSO pair of solvents. However, as the viscosity increased for H_2O/DMF, defects like junctions started to be seen except when 100% DMF was used. In the case of the DMF/DMSO solvent pair, thin fibers were observed in spite of a high solution viscosity when compared to H_2O/DMF. The mixture of these polar aprotic solvents with Pull even with high viscosity produce nanofibers with the smallest diameter and low variation on its values (220±30 nm). The difference of diameters of fibers obtained when electrospinning Pull/DMF/DMSO and Pull/H_2O/DMSO solutions, in spite of higher viscosity Pull/DMF/DMSO solutions, could be possibly, related, to the difference between hydrogen interactions between the binary mixtures. The Hansen interactions values of H_2O/DMSO and DMF/DMSO solvents with 30 wt.% of DMSO (Van Krevelen & Nijenhuis, 2009), the dispersion interactions (16.4 MPa$^{1/2}$ and 17.7g MPa$^{1/2}$) and polar interactions (16.1MPa$^{1/2}$ and 14.5 MPa$^{1/2}$) have reasonably close values. However, the hydrogen interactions show quite different values of 32.7 MPa$^{1/2}$ and 11.0 MPa$^{1/2}$.

The voltage used to electrospin Pull was also varied. Table 4 shows the average diameter of the fibers produced for 2 different voltages of 20kV and 24kV. It can be seen that the voltage does not seem to affect the diameter of the fibers except when the H_2O/DMF (30/70) was used which can be attributed to the presence of junctions, as already mentioned. It can also be seen that the smallest fibers diameters were obtained for DMF/DMSO solvent combination. This combination was taken when curcumin was added to the Pull.

Table 4. Average diameters (Ø) of the Pull fibers produced at 20 kV (1.2 kV/cm) and 24 kV (1.4 kV/cm) with different solvents.

Solution	Ø (nm)	Voltage (kV)
Pull/H$_2$O	302 ± 50	20
	340 ± 60	24
Pull/DMF	294 ± 37	20
	307 ± 56	24
Pull/H$_2$O/DMF (70/30)	320 ± 101	20
	303 ± 76	24
Pull/H$_2$O/DMF (30/70)	597 ± 154	20
	744 ± 196	24
Pull/H$_2$O/DMSO (70/30)	546 ± 82	20
	449 ± 80	24
Pull/DMF/DMSO (70/30)	220 ± 30	20
	203 ± 32	24

3.3. Effect of curcumin on the morphology of the nanofibers

Fig. 5 presents the morphology of these mats produced at 20 kV with (a) 3 wt.% and (b) 5 wt.% of Curc.
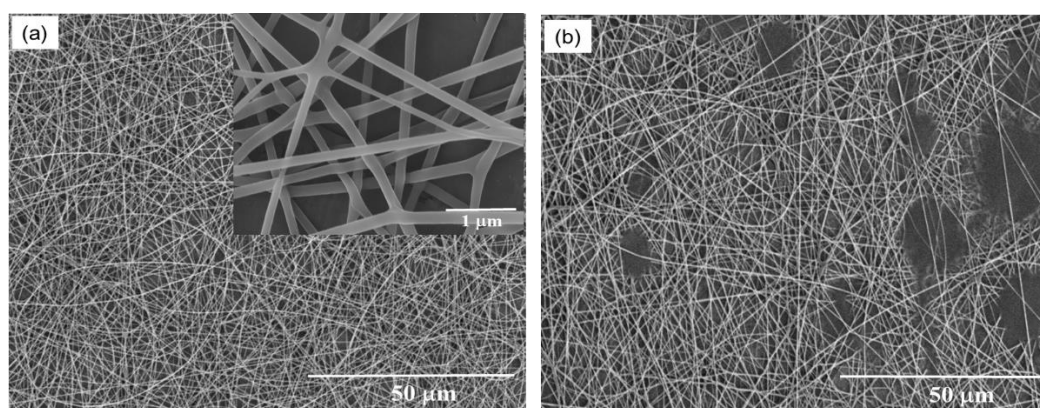

Figure 5. SEM morphology of the electrospun Pull produced at 20 kV with different Curc contents: (a) 3 wt.% and (b) 5 wt.%.

When 3 wt.% curcumin was added to the solution, smooth fibers were obtained (Fig. 5a). However, when 5 wt.% curcumin was added to the solution, some black beads were observed

(Fig. 5b), which can, possibly, be attributed to the curcumin not being incorporated in the fibers. These black beads were also obtained when 24 kV was used in both solutions (3 and 5 wt.%).

The viscosities of the solutions of Pull/DMF/DMSO with 3 and 5 wt.% of Curc have similar values which are 4,860 mPa.s and 4,920 mPa.s. These values are smaller than those for the solution without curcumin (10,940 mPa.s). The nanofibers containing 3 wt.% Curc were of smaller diameters, 155 ± 53 nm, than the ones without Curc (203 ± 32 nm), most likely due to the decrease of viscosity undergone by the solutions upon addition of Curc. The literature reports conflicting results showing that the influence of addition of Curc can either increase or decrease the diameter of the polymer fibers, meaning that it is highly dependent on the nature of the polymer. While Chen, Lin, Fei, Wang, and Gao (2010) found that the addition of Curc to PLA resulted in a decrease of fiber diameter and Blanco-Padilla, López-Rubio, Loarca-Piña, Gómez-Mascaraque, and Mendoza (2015) found that the addition of Curc to amaranth/Pull (50/50 wt.%) resulted in an increase of fiber diameter. Chen et al. (2010) also reported that the values of the conductivity of the solutions of Curc increased with the increase of the amount of Curc. Thus, Curc increases the conductivity of the solution and increases the velocity to split and the stretching of the jet during the electrospinning process, resulting in fibers with small diameters.

Entrapment efficiency of Curc in the Pull-Curc nanofiber mats was determined using the calibration plot of Curc in DMSO and was correlated with the results obtained by ^{1}H NMR and UV-vis analyses. Fig. 6 shows the ^{1}H NMR spectrum of Curc (a), Pull nanofibers (b) and Pull-Curc nanofibers (c). It can be seen that the acetyl protons ($-OCH_3-$) signals at 3.862 ppm from Curc and hydroxyl proton signals of Pull at 4.5-5.6 ppm are present in the spectra of Pull-Curc nanofibers (c) indicating that curcumin was entrapped within the fiber. As described in the literature, the presence of hydrophilic polymer favors the preservation of the Curc chemical structure (Yakub et al., 2020). A quantitative analysis was then performed, which indicated that 97.9 % of the Curc added to the solution was entrapped in the fibers. Quantitative UV-V analyses were, also, carried out and indicated that (95.4 ± 1.4) % of Curc was entrapped in the fibers. The results obtained in the present work are of the same order of magnitude as the ones obtained by Moorthy Ganeshkumar et al., (2016), who succeeded in entrapping 85.9 wt.% of Curc in Pull nanoparticles, and the ones of Wu, Tzeng, Lin, and Lin (2010) who succeeded in entrapping 99.3 wt.% in poly(vinylpyrrolidone) nanoparticles. These results indicate that the solvents and process used in this work enable the attainment of Pull nanofibers with curcumin.
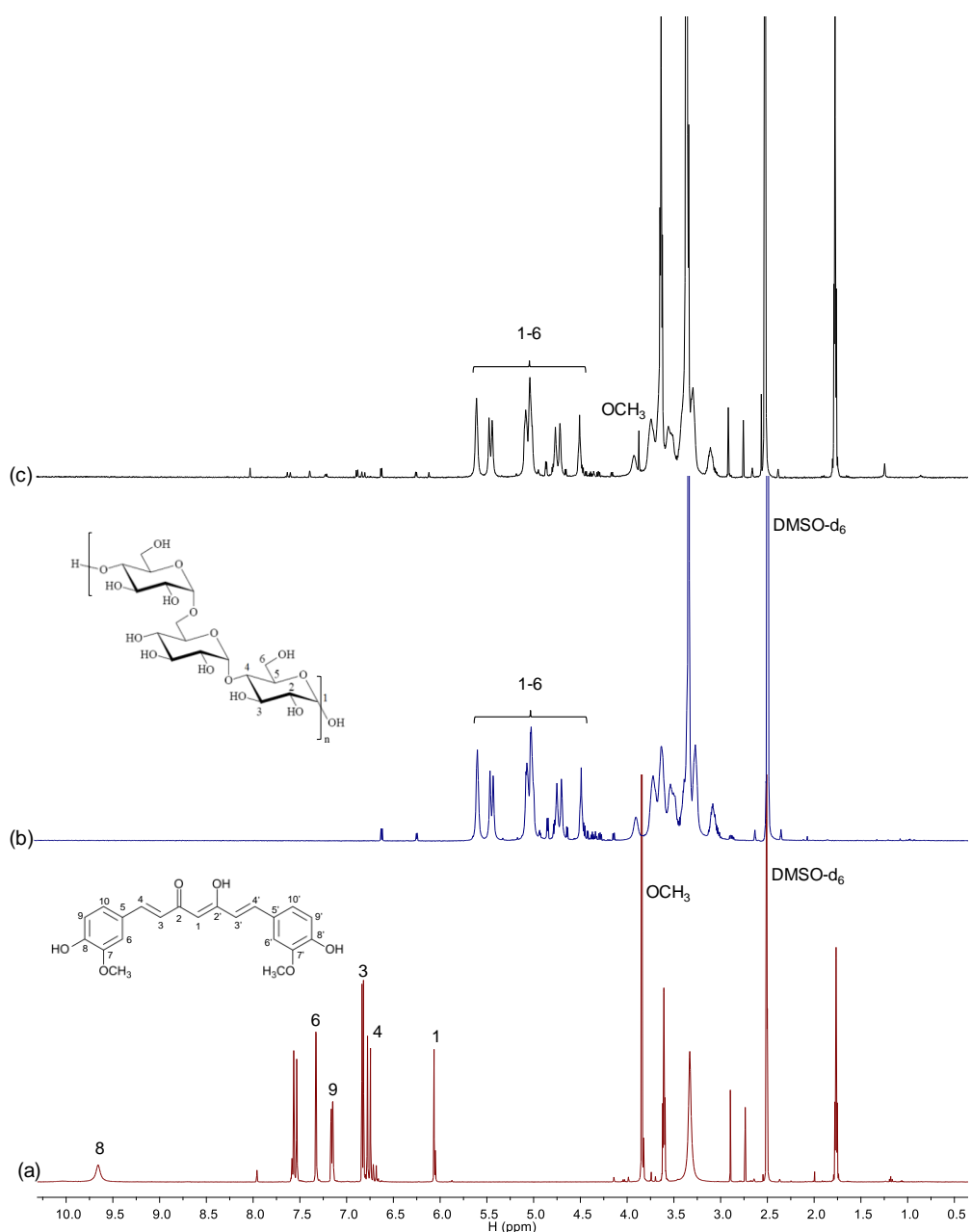
Figure 6. ^{1}H NMR spectra of Curc (a), Pull nanofibers (b) and Pull-Curc nanofiber mats from the DMSO/DMF solution containing 3 wt.% of Curc after being dissolved in DMSO-d6 (c).

4. Conclusions

In this work, the effect of the different solvents and solvent mixtures on the morphology of Pull electrospun nanofibers was, successfully, evaluated. Water, DMF and DMSO, as well as, several solvent mixtures were tested. It was possible to produce Pull mats without defects (beads and junctions) with water, DMF and the binary mixtures of water/DMSO and DMF/DMSO with 30 wt.% of DMSO. Using (DMF/DMSO) binary mixture as a solvent for Pull resulted in homogenous nanofibers with small diameters and narrow diameter distribution. The results indicated that the highest affinity between solvent and polymers (as evaluated using Teas graphs that rely on the use of solubility parameters) did not necessarily result in obtaining the most

15

homogeneous and finest fibers. The results indicate that the solution viscosity, boiling temperature, and electrical properties of the solvent, also, played a role in the possibility of obtaining fibers. When the boiling temperature of the solvent was too high, fibers would not have the time to dry before reaching the collector and, therefore, films were obtained. Pull nanofibers with 3 wt.% of curcumin were, also, produced without defects (beads and junctions) using a solvent mixture (DMF/DMSO) in the solution of 70/30 wt.% and 20 kV. The presence of curcumin resulted in a solution with small viscosity and electrospun nanofibers with diameters smaller than the Pull nanofibers without curcumin. The entrapment of curcumin in the nanofibers was around 98-96 wt.%, which showed that nanofiber of Pull with curcumin was efficient. The results obtained in this work created new approaches for the production of Pull nanofibers for drug delivery systems.

5. Acknowledgment

6. References

Balderrama, J. A. M., Dourges, M. A., Magueresse, A., Maheo, L., & Deleuze, H. (2018). Emulsion-templated pullulan monoliths as phase change materials encapsulating matrices. *Materials Today Communications*, *17*, 466-473. https://doi.org/10.1016/j.mtcomm.2018.10.012.

Bauer, R. (1938). Physiology of Dematium pullulans de Bary. *Zentralbl Bacteriol Parasitenkd Infektionskr Hyg Abt2, 98*, 133-167.

Bender, H., Lehmann, J., & Wallenfels, W. K. (1959). Pullulan, an extracellular glucan from Pullularia pullulans. *Biochimica et Biophysica Acta*, *36*, 309-316.

Blanco-Padilla, A., López-Rubio, A., Loarca-Piña, G., Gómez-Mascaraque, L. G., & Mendoza, S. (2015). Characterization, release and antioxidant activity of curcumin-loaded amaranth-pullulan electrospun fibers, *Food Science and Technology*, *63*,1137-1144.

Chen, Y., Lin, J., Fei, Y., Wang, H., & Gao. W. (2010). Membranes Preparation and characterization of electrospinning PLA/curcumin composite membranes. *Fibers and Polymers*, *11*, 1128-1131.

Cheng, K.C., Demirci, A., & Catchmark, J.M. (2011). Pullulan: Biosynthesis, production, and applications.. *Applied Microbiology and Biotechnology*, *92*, 29-44.

Ganeshkumar, M., Ponrasu, T., Subamekala, M. K., Janani, M., & Suguna, L. (2016). Curcumin loaded on pullulan acetate nanoparticles protects the liver from damage induced by DEN. *RSC Advances, 6,* 5599-5610. https://doi.org/10.1039/C5RA18989F.

Guerrini, L.M., Oliveira, M.P., Branciforti M.C., Custódio, T.A., & Bretas, R.E.S. (2009). Thermal and structural characterization of nanofibers of poly(vinyl alcohol) produced by electrospinning. *Journal of Applied Polymer Science. 112*, 1680-1687.

Han, T., Yarin, A. L., & Reneker, D. H. (2008). Viscoelastic electrospun jets: Initial stresses and elongational rheometry, *Polymer*, *49*, 1651-1658.

Hansen, C. M., (1967a). The three dimensional solubility parameter-key to paint component affinities: III. Independent calculation of the parameters components, *Journal of Paint Technol. 39*, 511–514.

Hansen, C.M. (1967b). The three dimensional solubility parameter-key to paint component affinities: I. Solvents, plasticizers, polymers, and resins. Journal of Paint Technol, 39, 104–117.

Hansen, C.M. (1967c). The three dimensional solubility parameterkey to paint component affinities: II. Dyes, emulsifiers, mutual solubility and compatibility and pigments. Journal of Paint Technol., 39, 505–510.

Hilares, R. T., Resende, J., Orsi, C. A., Ahmed, M. A., Lacerda, T. M., Silva, S. S., & Santos, J. C. (2019). Exopolysaccharide (pullulan) production from sugarcane bagasse hydrolysate aiming to favor the development of biorefineries. *International Journal of Biological Macromolecules*, *127*, 169-177. https://doi.org/10.1016/j.ijbiomac.2019.01.038.

Hildebrand, J. H., & Scott, R. L. (1962). *Regular solutions*. New York: Prentice-Hall, Englewood Cliffs.

Ilić, L. J., Jeremi, K., & Jovanovi, S. (1991). Acid Kinetics of pullulan depolimerization in hydrochloric acid., *European Polymer Journal. 27*, 1227-1229.

Jo, J. I., Ikai, T., Okazaki, A., Yamamoto, M., Hirano, Y., & Tabata, Y. (2007). Expression profile of plasmid DNA by spermine derivatives of pullulan with different extents of spermine introduced. *Journal of Controlled Release. 118*, 389-398.

Kong, L., Ziegler, G. R. (2014). Rheological aspects in fabricating pullulan fibers by electro-wetspinning, *Food Hydrocolloids*, 38, 220-226.

Kumar, D., Saini, N., Pandit, V., & Ali, S. (2012). An insight to pullulan: A biopolymer in pharmaceutical approaches. *International Journal of Basic and Applied Sciences, 1*, 202-219.

Leathers, T. D. (2003). Biotechnological production and applications of pullulan. *Applied Microbiology and Biotechnology*, 62*,* 468-473.

López-Rubio, A., Sanchez, E., Wilkanowicz, S., Sanz, Y., & Lagaron, J. M. (2012). Electrospinning as a useful technique for the encapsulation of living bifidobacteria in food hydrocolloids, *Food Hydrocolloids*, *28*, 159-167.

Lubasova, D., Martinova, L. (2011). Controlled morphology of porous polyvinyl butyral nanofibers, *Journal of Nanomaterials*, ID 292516, https://doi.org/10.1155/2011/292516.

Luo, C. J., Stride, E., & Edirisingh, M. (2012). Mapping the influence of solubility and dielectric constant on electrospinning polycaprolactone solutions. *Macromolecules*, *45*, 4669-4680.

Mahalingam, S., Raimi-Abraham, B., Craig, D. Q. M., & Edirisinghe, M. (2015). Solubility-spinnability map and model for the preparation of fibres of polyethylene (terephthalate) using gyration and pressure, *Chemical Engineering Journal*, 280, 344-353.

Mark, J. E. (ed). Polymer data handbook, 1999: Oxford University Press.

Oguzhan, P., & Yangilar, F. (2013). Pullulan production and usage in food industry. *African Journal of Food Science and Technology, 4*, 57-63.

Pereira, J. M. Synthesis of new pullulan derivatives for drug delivery, PhD dissertation, Virginia Polytechnic Institute and State University, 2013.

Prajapati, V. D., Jani, G. K., & Khanda, S. M. (2013). Pullulan: Na exopolysaccharide and its various applications. *Carbohydrate Polymer*, *95*, 540-549. https://doi.org/10.1016/j.carbpol.2013.02.082

Rekha, M. R., & Sharma, C. P. (2007). Pullulan as a promising biomaterial for biomedical applications: A Perspective. *Trends in Biomaterials & Artificial Organs*, *20*, 111-116.

Rezaei A., Nasirpour A. (2019). Evaluation of Release Kinetics and Mechanisms of Curcumin and Curcumin-β-Cyclodextrin Inclusion Complex Incorporated in Electrospun Almond Gum/PVA Nanofibers in Simulated Saliva and Simulated Gastrointestinal Conditions. *Bionanoscience*, 9, 438-445.

Senthil, T., & Anandhan, S. (2013). Solution electrospinning of styrene-acrylonitrile random copolymer from dimethyl sulfoxide. *International Journal of Plastics Technology*. *17*, 123-138.

Shady, S. F., Gaines, P., Garhwal, R., Leahy, C., Ellis, E., Crawford, K., Schmidt, D. F., & McCarthy, S. P. (2013). Synthesis and characterization of pullulan-polycaprolactone core–shell nanospheres encapsulated with ciprofloxacin., *Journal of Biomedical and Nanotechnol*ogy, *9*, 1644-1655. https://doi.org/10.1166/jbn.2013.1654.

Singh, R. S.; Kaur, N., & Kennedy, J. F. (2015). Pullulan and pullulan derivatives as promising biomolecules for drug and gene targeting. *Carbohydrate Polymer*, *123*, 190-207. https://doi.org/10.1016/j.carbpol.2015.01.032

Smallwood, I. M. Handbook of organic solvent properties, 1996: John Wiley & Sons.

Stijnman, A. C., Bodnar I., & Tromp R. H. (2011). Electrospinning of food-grade polysaccharides, *Food Hydrocolloids*. *25*, 1393-1398.

Sugumaran, K. R., & Ponnusami, V. (2017). Review on production, downstream processing and characterization of microbial pullulan. Carbohydrate Polymers, 173, 573-59. http://dx.doi.org/doi:10.1016/j.carbpol.2017.06.022.

Sun, X., Williams, G. R., Hou, X., & Zhu, L. (2013). Electrospun curcumin-loaded fibers with potential biomedical applications, *Carbohydrate Polymers*, *94*, 147-153.

Swn, Y.C., Kim, Y.H., Lee. H.S.; Cho, S., & Bvum. S.M. (1989). Production of exopolysaccharide pullulan from inulin by a mixed culture of *Aureobasidium pullulans* and *Kluyveromyces fragilis*. *Biotechlology and Bioengineering*, 33, 129-133.

Tabasum, S., Noreen, A., Maqsood, M. F., Umar, H., Akram, N., Nazli, Z., Ali, S., Chatha, S., & Zia, K. M. (2018). *International Journal of Biological Macromolecules,* 120, 603-632, 2018. https://doi.org/10.1016/j.ijbiomac.2018.07.154.

Tsujisaka, Y., Mitsuhashi, M. Pullulan. In R. L. Whistler & J. N. BeMiller (Eds.), *Industrial gums, polysaccharides and their derivatives* (p. 447-460). San Diego, CA: Academic Press, 1993.

Van Krevelen, D. W., Nijenhuis, K. (2009). Properties of polymers – Their correlation with chemical structure and numerical estimation and prediction from additive group contributions. Cohesive properties and solubility (fourth edition). Nethelands, Elsevier Ed., 898p.

Willersinn J., Bogomolova A., Cabré M. B., Schmidt B. V. K. J. (2017). Vesicles of double hydrophilic pullulan and poly(acrylamide) block copolymers: A combination of synthetic- and bioderived blocks, *Polymer Chemistry*, 8, 1244-1254.

Yakub, G., Toncheva, A., Kussovski, V., Toshkova, R., Georgieva, A., Nikolova, E., Manolova, N., & Rashkov, I. (2020). Curcumin-PVP loaded electrospun membranes with conferred antibacterial and antitumoral activities. *Fibers and Polymers*, *21*, 55-65. https://doi.org/10.1007/s12221-020-9473-z.

Yakub, G., Toncheva, A., Kussovski, V., Toshkova, R., Georgieva, A., & Nikolova, E., et al. (2020). *Fibers and Polymers*, 21, 55–65.

Yen, F.L, Wu, T.H., Tzeng,C.W., Lin,L.T., Lin,C.C. (2010). Curcumin nanoparticles improve the physicochemical properties of curcumin and effectively enhance its antioxidant and antihepatoma activities. Journal of Agricultural and Food Chemistry, 58, 7376-7382.